Planetary and Space Science 59 (2011) 402–411

Contents lists available at ScienceDirect

Planetary and Space Science

journal homepage: www.elsevier.com/locate/pss

MHD-instability of the magnetotail: Global modes

A.S. Leonovich *

Institute of Solar-Terrestrial Physics, SB RAS, P.O. Box 291, Irkutsk 664033, Russia

ARTICLE INFO

Article history:
Received 22 July 2010
Received in revised form
11 January 2011
Accepted 11 January 2011
Available online 18 January 2011

Keywords:
Magnetotail
MHD waves
Instability
Global modes

ABSTRACT

A hydromagnetic stability problem is solved for the magnetospheric tail inside the solar wind plasma flow. A model magnetotail is used in the form of a plasma cylinder which is inhomogeneous over the radius. For a qualitative analysis of the problem the solution is obtained analytically, in the WKB approximation. The plasma cylinder boundary is assumed to have the form of a tangential discontinuity. A numeric solution was found for a more realistic model, with the boundary in the form of a smooth transition layer. This model cannot simulate such a feature of the actual magnetotail as its being divided into two lobes with opposite magnetic fields. It is capable, however, of simulating the finiteness of the magnetotail cross-section and the inhomogeneous plasma distribution over the radius. It is shown, analytically, that a local instability develops in the boundary when the velocity of the plasma flowing round the magnetosphere exceeds the Alfvén speed at the magnetotail boundary. This conclusion is supported by a numerical solution of the problem for a model with its boundary in the form of a smooth transition layer. The instability increment, however, is much smaller in the latter case. Apart from a local instability of the boundary, unstable global modes are discovered whose amplitude practically does not vary over the magnetotail cross-section. These modes remain unstable for any, however, slow velocities of the plasma flowing round the magnetosphere. When the plasma flow velocity reaches a critical magnitude the global modes of the MHD oscillations become stable. Unstable global modes may be a source of ultra-low-frequency ($\sim$1 mHz) oscillations observed in the Earth's nightside magnetosphere.

1. Introduction

Many low-frequency MHD oscillations in the Earth's and other solar-system planets' magnetospheres are associated with a shear plasma flow instability developing at the magnetospheric boundary (Kelvin–Helmholtz instability) Engebretson et al. (1998). A number of papers have been devoted to observations of the oscillations treated as such unstable modes (see Mann and Wright, 1999; Mann et al., 2002, etc.), and to their theoretical interpretation (see Southwood, 1968; McKenzie, 1970a; Mills et al., 1999, etc.). A mechanism related to the resonator for fast magnetosonic waves in the near-Earth part of the plasma sheet was proposed and theoretically developed in recent papers (Leonovich and Mazur, 2005; Mazur and Leonovich, 2006) for ultra-low-frequency oscillations with a discrete spectrum (so-called "magic frequencies"—0.8, 1.1, 1.6 …mHz) forming in the magnetosphere. However, part of the wave energy escapes from this resonator to the solar wind Leonovich and Mazur (2008). Therefore, a rather powerful source is required to be present in order to drive the eigen-modes in such a resonator. Magnetotail instability resulting from the solar wind flowing around the magnetotail has been suggested as a possible source.

In this paper we will use a rather simple plasma-cylinder model of the magnetotail in an attempt to calculate theoretically the increment of such an instability. The majority of the theoretical papers deal with models of the medium that have the form of two homogeneous half-spaces divided by a shear flow layer (see McKenzie, 1970a; Rankin et al., 1997). Such models allow one to obtain analytical solutions to MHD equations, which, unfortunately, have a rather weak relation to the real magnetosphere.

Actual magnetospheres are very inhomogeneous, which adds specific aspects to the conditions for an instability to develop in such plasma systems. The plasma sheet divides the magnetotail cross-section into two lobes with directly opposite magnetic field. This results in both radial and azimuthal inhomogeneity in the magnetotail. It is also longitudinally inhomogeneous, which undoubtedly results in certain peculiarities in the instability development. Unfortunately, no methods have so far been developed for a rigorous solution of the hydromagnetic stability problem in two- or three-dimensional inhomogeneous magnetotail models (barring the numerical simulation methods). Far from everything has been done, however, even in problems based on

* Tel.: +7 89148979925; fax: +7 83952511675.
E-mail address: leon@iszf.irk.ru

0032-0633/$ - see front matter © 2011 Elsevier Ltd. All rights reserved.
doi:10.1016/j.pss.2011.01.006

one-dimensional-inhomogeneous models. The real magnetosphere features a number of properties which have not yet been addressed, but which can be taken into account even while using a one-dimensional-inhomogeneous model to solve the problem.

Their essential feature is the presence of resonance surfaces for the Alfvén and slow magnetosonic waves where MHD oscillation energy is absorbed (Leonovich and Kozlov, 2009). The instability develops in the boundary transition layer near the surface where the parallel component of the MHD-wave phase velocity is equal to the velocity of plasma flowing round the magnetosphere. The magnetotail stability is determined by competition between two effects—an instability developing in the transition layer and MHD oscillation energy absorbed on the resonance surfaces. Few papers have so far managed to address these two effects (Fujita et al., 1996). Those papers also deal with models of the medium in the form of two half-spaces divided by a transition layer with a shear plasma flow. One of the half-spaces, simulating the magnetosphere, is assumed to be inhomogeneous.

Another feature should be taken into account when modelling the MHD instability in the magnetosphere in the solar wind flow—the finite size of the magnetospheric cross-section in the plasma flow. The problem has been solved in McKenzie (1970b) for a magnetospheric model in the form of a plasma cylinder. The plasma in the model magnetosphere, however, was assumed to be homogeneous, which precluded any resonant coupling of various MHD modes on the resonance surfaces.

This paper will use an inhomogeneous plasma cylinder model to solve the magnetotail stability problem. This will allow both the finiteness of the magnetotail cross-section and the presence of resonance surfaces for Alfvén and SMS waves to be taken into account. For a qualitative analysis the problem was solved analytically for oscillations that could be described using the WKB approximation over the radial coordinate. The boundary of the plasma cylinder was assumed to have the form of a tangential discontinuity. For a more realistic model with the boundary in the form of a smoothly varying transition layer, the problem was solved numerically. It turned out that, along with local unstable modes of the magnetospheric boundary, such a plasma system also exhibits unstable "global modes" whose amplitude practically does not vary across the magnetotail. Such oscillations can be a source of ultra-low-frequency MHD oscillations of the magnetospheric resonator in the near-Earth part of the plasma sheet. Whether these solutions can be applied to the real magnetosphere remains questionable. It is an inevitable problem which can only be resolved using more precise two- or three-dimensional- inhomogeneous models when appropriate methods for their solutions appear.

The paper is structured as follows. The model of the medium is presented and the basic equations describing MHD oscillations in a moving plasma, in cylindrical geometry, are obtained in Section 2. The instability increment of the magnetotail boundary is calculated in the WKB approximation in Section 3. The stability problem of a magnetotail with a smooth boundary is solved numerically in Section 4. The instability of global modes in the magnetotail is examined in Section 5. The Conclusion lists the main results of the work.

2. The model of the medium and basic equations

Let us consider a model magnetospheric tail in the form of an inhomogeneous plasma cylinder, as shown in Figs. 1 and 2. The plasma distribution over the radius corresponds to the magnetotail lobes. This model does not explicitly include the plasma sheet of the actual magnetosphere. Its presence is simulated by the Alfvén speed and sound velocity distribution over the radius. When moving away

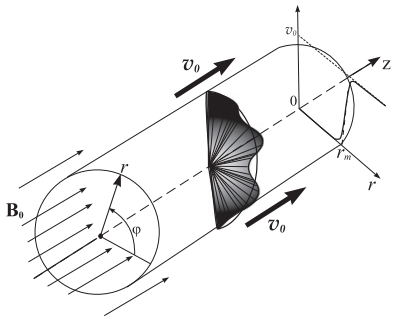

Fig. 1. A cylindrical model of the magnetotail within the solar wind plasma flow. Magnetic field is along the plasma cylinder axis. The amplitude distribution of "global mode" oscillations in one of the magnetotail sectors is shown schematically.

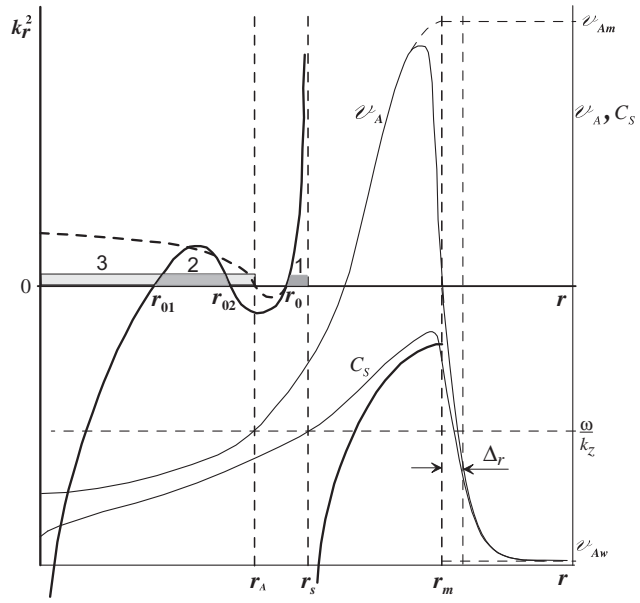

Fig. 2. Distribution of the Alfvén speed $v_A(r)$ and SMS velocities $C_s(r)$ in the magnetotail and in the solar wind (thin lines, right-hand vertical axis). Distribution of the square of the WKB component $k_r^2(r)$ of the wave vector over the magnetotail radius (thick lines; dashed for the mode $m=0$; left-hand vertical axis). Numerals and shades of gray denote the transparency regions: (1) for the SMS waves, (2) for the FMS waves with $m\neq 0$ and (3) for the FMS waves with $m=0$.

from the cylinder axis their magnitudes change from those typical in the plasma sheet to those typical in the magnetotail lobes. As has already been noted in the Introduction, the issue of whether the results obtained here in the framework of a one-dimensionally inhomogeneous model can be applied to the real magnetosphere may only be answered dealing with two- or three-dimensionally inhomogeneous models. Presumably, the results obtained in this paper are qualitatively applicable to describing the MHD instability in each magnetotail lobe.

The local instability of the magnetotail boundary is determined by the parameters of the directly adjoining magnetospheric and solar wind regions. The instability of the global modes, on the other hand, is determined by the integral properties of the magnetotail plasma and does not depend on specific details of the plasma distribution over the radius. The presence of an azimuthal or longitudinal inhomogeneity must, of course, considerably modify the expression for the increment of these modes, but we hope that it will not affect their very existence.

We specify a cylindrical coordinates system (r,ϕ,z), where the origin $r=0$ coincides with the plasma cylinder axis. We will

assume the background magnetic field to be homogeneous in (but not identical between) the magnetotail and the solar wind and to be directed along the z axis. In our analytical calculations we will use the m subscript to denote the parameters of the medium at the plasma cylinder boundary ($r=r_m$) on the magnetospheric side, while using w for the solar wind side. We will assume the solar wind plasma to be moving at velocity v_0 along the z axis, while deeming the magnetotail plasma to be immobile (see Fig. 1).

The transition from the magnetospheric to the solar wind parameters takes place in a narrow transition layer of thickness $\Delta_r \ll r_m$. We will deem the plasma density distribution over the radius to be such that its maximum should be at the plasma cylinder axis decreasing to a minimum on the cylinder boundary. The magnetic field in the magnetotail is stronger than in the solar wind. Qualitatively, the distribution of the Alfvén speed $v_A = B_0/\sqrt{\mu_0\rho_0}$ (where μ_0 is the permeability of the vacuum) over the radius has the form illustrated in Fig. 2. Such a distribution of parameters is typical for the plasma of the Earth's magnetotail lobes. The averaged distribution of the Alfvén speed in the magnetosphere under medium-disturbed conditions in the equatorial and meridional (along the noon-midnight meridian) cross-sections based on satellite data (Sergeev and Tsyganenko, 1980; Borovsky et al., 1998) was presented in Mazur and Leonovich (2006).

To describe the oscillations, let us use the ideal MHD equation set of the form

$$\rho\frac{d\overline{\mathbf{v}}}{dt} = -\nabla\overline{P} + \frac{1}{\mu_0}[\mathrm{curl}\overline{\mathbf{B}}\times\overline{\mathbf{B}}], \tag{1}$$

$$\frac{\partial\overline{\mathbf{B}}}{\partial t} = \mathrm{curl}[\overline{\mathbf{v}}\times\overline{\mathbf{B}}], \tag{2}$$

$$\frac{\partial\overline{\rho}}{\partial t} + \mathrm{div}(\overline{\rho}\,\overline{\mathbf{v}}) = 0, \tag{3}$$

$$\frac{d}{dt}\frac{\overline{P}}{\overline{\rho}^{\gamma}} = 0, \tag{4}$$

where $\overline{\mathbf{B}},\overline{\mathbf{v}}$ are the vectors of magnetic field and plasma motion velocity, $\overline{\rho},\overline{P}$ are the plasma density and pressure, $\gamma=\frac{5}{3}$ is the adiabatic index. Let us assume that the wave-related disturbance is rather weak, allowing the initial set of equations to be linearised. Let us use the zero subscript to denote the parameters referring to undisturbed plasma, while leaving the wave-related parameters unindexed ($\overline{P}=P_0+P, \overline{\rho}=\rho_0+\rho, \overline{\mathbf{B}}=\mathbf{B_0}+\mathbf{B}, \overline{\mathbf{v}}=\mathbf{v}_0+\mathbf{v}$). In the zero approximation the r component of Eq. (1) yields ($\partial/\partial t=0$) the equilibrium condition of the plasma configuration in a steady state

$$P_0 + \frac{B_0^2}{2\mu_0} = const, \tag{5}$$

which determines the equilibrium distribution of the plasma pressure $P_0(r)$ for the given distribution of $B_0(r)$. This pressure determines the sound velocity distribution in plasma $v_s=\sqrt{\gamma P_0/\rho_0}$ and the corresponding distribution of the velocity of slow magnetosonic (SMS) waves $C_s = v_A v_s/\sqrt{v_A^2+v_s^2}$ in Fig. 2. Let us assume that the magnetic field strengths are almost constant in the magnetotail and in the solar wind, changing only in the thin transition layer of thickness $\Delta_r \ll r_m$. The following values were used in the numerical calculations: $r_m=30$ Re, $\Delta_r=2$ Re, where Re=6370 km is the typical radius of the Earth. The equilibrium condition (5) implies that the plasma pressure also varies inside the transition layer only. The background plasma and magnetic field parameter values at the magnetotail boundary used in the following numerical calculations are listed in Table 1. These parameters satisfy the equilibrium condition (5) of the plasma configuration.

Table 1
Main parameters of the medium at the magnetotail boundary.

Parameter	Region	
	Magnetotail lobes	Solar wind
B_0 (nT)	20	5
v_A (km/s)	6000	50
v_s (km/s)	420	177
$\beta^*=v_s^2/v_A^2$	0.005	12.6

Let us denote the r-axis component of the vector of the disturbed plasma velocity in the wave as $v_r = \mathrm{d}\zeta/\mathrm{d}t = \partial\zeta/\partial t + (\mathbf{v}_0\nabla)\zeta$, where ζ is displacement of the plasma element. Let us consider a simple harmonic wave of the form $\exp(ik_z z + im\phi - i\omega t)$, where k_z is the wave vector component in the z axis direction, $m=0,1,2,3\ldots$ is the azimuthal wave number, ω is wave frequency. Linearizing the set of Eqs. (1)–(4) and expressing the other components of the oscillation field through ζ produces (see Appendix A):

$$v_r = -i\overline{\omega}\zeta, \quad v_\phi = -\frac{1}{K_s^2}\left(v_A^2 + \frac{K_A^2 v_s^2}{\chi_S^2}\right)\frac{m}{\overline{\omega}r^2}\frac{\partial r\zeta}{\partial r},$$

$$v_z = -\frac{k_z K_A^2 v_s^2}{\overline{\omega}\chi_S^2 r}\frac{\partial r\zeta}{\partial r} - \zeta\frac{dv_0}{dr}, \tag{6}$$

$$B_r = -ik_z B_0\zeta, \quad B_\phi = -\frac{k_z B_0}{\overline{\omega}}v_\phi,$$

$$B_z = -\frac{K_A^2 B_0}{\chi_S^2}\left(1 - \frac{k_z^2 v_s^2}{\overline{\omega}^2}\right)\frac{1}{r}\frac{\partial r\zeta}{\partial r} - \zeta\frac{dB_0}{dr}, \tag{7}$$

$$P = -\gamma P_0\frac{K_A^2}{\chi_S^2}\frac{1}{r}\frac{\partial r\zeta}{\partial r} + \zeta\frac{d}{dr}\left(\frac{B_0^2}{2\mu_0}\right), \tag{8}$$

where the notations are

$$K_A^2 = 1 - \frac{k_z^2 v_A^2}{\overline{\omega}^2}, \quad K_s^2 = K_A^2 - \frac{m^2 v_A^2}{r^2\overline{\omega}^2},$$

$$\chi_S^2 = 1 - \frac{m^2/r^2 + k_z^2}{\overline{\omega}^2}\left(v_A^2 + v_s^2 - \frac{k_z^2 v_A^2 v_s^2}{\overline{\omega}^2}\right),$$

$\overline{\omega} = \omega - k_z v_0$ is the oscillation frequency modified by Doppler's effect. For displacement ζ we obtain

$$\frac{\partial}{\partial r}\left(\frac{\rho_0\Omega^2}{k_r^2}\frac{1}{r}\frac{\partial r\zeta}{\partial r}\right) + \rho_0\Omega^2\zeta = 0, \tag{9}$$

where $\Omega^2 = \overline{\omega}^2 - k_z^2 v_A^2$,

$$\begin{aligned} k_r^2 &= \frac{\overline{\omega}^4}{\overline{\omega}^2(v_A^2+v_s^2) - k_z^2 v_A^2 v_s^2} - k_z^2 - \frac{m^2}{r^2} \\ &= k_z^2\left(\frac{\overline{\omega}_A^4/(1+\beta^*)}{(\overline{\omega}_A^2 - \overline{\omega}_S^2)} - 1 - \frac{m^2}{k_z^2 r^2}\right) \\ &= \frac{k_z^2}{1+\beta^*}\frac{(\overline{\omega}_A^2 - \overline{\omega}_{A1}^2)(\overline{\omega}_A^2 - \overline{\omega}_{A2}^2)}{(\overline{\omega}_A^2 - \overline{\omega}_S^2)}, \end{aligned} \tag{10}$$

and $\overline{\omega}_A = \overline{\omega}/k_z v_A(r)$, $\overline{\omega}_S = \sqrt{\beta^*/(1+\beta^*)}$, $\beta^* = v_s^2/v_A^2$, and $\overline{\omega}_{A1}^2, \overline{\omega}_{A2}^2$ are the roots of biquadratic (with respect to $\overline{\omega}_A$) equation $k_r^2=0$. Note that the expression β^* coincides, within a factor close to unity, with the well-known parameter $\beta = 2\mu_0 P_0/B_0^2$—the ratio of gas-kinetic pressure of plasma to magnetic pressure. One can see from (9) that k_r^2 is the square of the r component of the wave vector in the WKB approximation if the solution of (9) can be presented in the form $\zeta \sim \exp(i\int k_r dr)$.

A WKB solution of the problem is determined by the magnitude of the k_r component of the wave vector on both sides of the boundary (having the form of a tangential discontinuity). Let us qualitatively analyse the behaviour of $k_r^2(r)$ in the above model magnetotail. The distribution of $k_r^2(r)$ in the plasma cylinder is qualitatively shown in Fig. 2. The figure shows the distribution of $k_r^2(r)$ for such values of parameters m, k_z and ω for which all possible resonance surfaces and turning points are present in the magnetotail.

The turning points are determined by zeros of the function $k_r^2(r)$. In the distribution in Fig. 2 their number can vary from one (r_0) to three (r_0, r_{01}, r_{02}). The number of turning points is determined by the values of the parameters m, k_z and ω. Thus, for the axisymmetric mode $m=0$ the turning point r_{02} is absent, while point r_{01} coincides with point r_A which is a resonance surface for the Alfvén waves when $m\neq 0$. The resonance surfaces are determined by the singular points of Eq. (9), where the coefficient for the higher derivative becomes zero.

The Alfvén resonance point r_A, determined by equality $\Omega^2(r_A)=0$, is located in the opacity region in the interval (r_{02}, r_0). When $m=0$, r_A is a turning point (the coefficient for the higher derivative is not zero at the point). The magnetosonic resonance point r_s is determined by the denominator in expression (10) becoming zero, yielding the local dispersion equation for SMS waves when $|k_r^2|\to\infty$: $\omega^2=k_z^2C_s^2(r_s)$.

For fast magnetosonic (FMS) waves, a transparency region (where $k_r^2(r)>0$) can exist in the magnetotail, which for $m\neq 0$ is located in the range $r_{01}\le r\le r_{02}$, and for $m=0$ – in the range $0\le r\le r_A$. The transparency region for SMS waves is located in the range $r_0\le r\le r_s$ (where r_s is the resonance surface for SMS oscillations). It is evident from (10) that the behaviour of $k_r^2(r)$ in the range $0<r<r_m$ depends on the magnitude of $\overline{\omega}_A(r)$ at its ends. The distribution of $k_r^2(r)$ depending on increasing phase velocity ω/k_z of the wave under consideration may be imagined by mentally moving the function $k_r^2(r)$ in Fig. 2 from left to right. When $\omega/k_z\to 0$ the entire magnetosphere is the opacity region corresponding to the part in the plot where $r_s<r<r_m$, and when $\omega/k_z\to\infty$ the magnetosphere is a transparency region corresponding to the part $r_{01}<r<r_{02}$ for $r_{01}\to 0$ and $r_{02}>r_m$. Depending on the magnitudes of $\overline{\omega}_{Am}^2$ and $\overline{\omega}_{Aw}^2$, determined by wave phase velocity, the boundary can be adjoined either by the transparency or opacity regions of the oscillations under study.

The matching condition at the boundary is easily obtained for the solution by integrating Eq. (9) within a narrow interval $(r_m-\varepsilon, r_m+\varepsilon)$ for $\varepsilon\to 0$:

$$\left.\frac{\rho_0\Omega^2}{k_r^2}\frac{\partial\ln(\zeta)}{\partial r}\right|_{r_m-\varepsilon}=\left.\frac{\rho_0\Omega^2}{k_r^2}\frac{\partial\ln(\zeta)}{\partial r}\right|_{r_m+\varepsilon}. \tag{11}$$

Using expressions (7) and (8) it is possible to show that (11) is similar to the requirements that the plasma should be identically displaced on both sides of the boundary ($\zeta_{r_m-\varepsilon}=\zeta_{r_m+\varepsilon}$ is the condition of impermeability) and that the total perturbed pressure should remain the same across the boundary ($(P+B_zB_0/\mu_0)_{r_m-\varepsilon}=(P+B_zB_0/\mu_0)_{r_m+\varepsilon}$).

Let us now determine the boundary conditions for the problem to be solved. When $r\to 0$ the boundary condition is the requirement for the desired solution to be finite. When $r\to\infty$ the boundary condition is determined by the causality principle. In this problem we are interested in the solutions of (9) describing the unstable modes of oscillations. Such solutions, according to the causality principle, describe waves escaping from the shear flow that generates them. In other words, the energy flux of these waves should be directed away from the shear layer. Notably, the k_r component of the wave vector of unstable oscillations is complex in the asymptotically far regions. For any unstable oscillations, it is formally possible to introduce the concept of waves escaping from the shear layer with $\mathrm{Re}(v_{gr})>0$ when $r\to\infty$, where $v_{gr}=\partial\omega/\partial k_r$ is the group velocity at which the wave energy is transported over radius r. The energy conservation law for monochromatic unstable ($\mathrm{Im}(\omega)>0$) oscillations

$$\frac{\partial\mathcal{E}}{\partial t}+\frac{1}{r}\frac{\partial}{\partial r}(r\mathbf{v}_{gr}\mathcal{E})=0,$$

results in $\mathrm{Im}(k_r)>0$ when $r\to\infty$, where $\mathcal{E}$ is oscillation wave energy density (which is quadratic in amplitude). This provides for an exponentially decreasing amplitude of oscillations escaping from the shear layer. A specific expression for the group velocity when $r\to\infty$ can be obtained by means of differentiating the expression (10) with respect to ω:

$$v_{gr}=v_{A\infty}\frac{1+\beta_\infty^*}{k_z}\mathrm{Re}(k_{r\infty})\frac{[\overline{\omega}_{A\infty}^2-\overline{\omega}_{S\infty}^2]^2}{\overline{\omega}_{A\infty}^3[\overline{\omega}_{A\infty}^2-2\overline{\omega}_{S\infty}^2]}. \tag{12}$$

The boundary condition for a wave escaping from the shear layer when $r\to\infty$ is

$$\frac{\partial\zeta}{\partial r}=ik_{r\infty}\zeta, \tag{13}$$

and the sign of $k_{r\infty}\equiv k_r(r\to\infty)=\pm\sqrt{k_{r\infty}^2}$ is determined by the requirement $\mathrm{Re}(v_{gr})>0$.

3. WKB calculation of magnetotail boundary instability increment

To understand qualitatively how the increment of unstable oscillations in the magnetotail boundary depends on the speed of the solar wind flux flowing round the magnetotail, let us use WKB approximation over the r coordinate to tackle the problem. Let us employ such parameter sets of unstable oscillations for which their resonance surfaces and turning points are located far from the boundary $r=r_m$, and the WKB approximation is applicable for the nearby oscillations. If the oscillations are weakly unstable ($|\mathrm{Re}(\omega)|\gg|\mathrm{Im}(\omega)|$), let us regard the region adjoining the boundary as an opacity region if $\mathrm{Re}(k_r^2(r_m))<0$, or as a transparency region if $\mathrm{Re}(k_r^2(r_m))>0$. If the transparency region adjoins the magnetotail boundary on the solar wind side ($r>r_m$), the solution of (9) for an unstable mode in the solar wind is a wave escaping from the boundary. Its WKB solution is

$$\zeta=C_w\sqrt{\frac{k_r}{\rho_0\Omega^2 r}}\exp\left(i\int_{r_m}^{r}k_r\,dr'\right), \tag{14}$$

where C_w is an arbitrary constant. If, however, the solar wind is opaque, the solution looks like a surface wave decreasing in amplitude from the boundary towards the solar wind

$$\zeta=C_w\sqrt{\frac{k_r}{\rho_0\Omega^2 r}}\exp\left(-\int_{r_m}^{r}\sqrt{-k_r^2}\,dr'\right). \tag{15}$$

Similarly, if the opacity region adjoins the boundary on the magnetospheric side ($r<r_m$) the WKB solution of (9) looks like a surface wave with its amplitude decreasing into the magnetosphere

$$\zeta=C_m\sqrt{\frac{k_r}{\rho_0\Omega^2 r}}\exp\left(\int_{r_m}^{r}\sqrt{-k_r^2}\,dr'\right). \tag{16}$$

If, however, the transparency region adjoins the boundary on the magnetotail side, the WKB solution on the magnetospheric side is

$$\zeta=C_m\sqrt{\frac{k_r}{\rho_0\Omega^2 r}}\cos\left(\int_{r_m}^{r}k_r\,dr'+\psi\right), \tag{17}$$

where $\psi=\int_{r_{00}}^{r_m}k_r dr+\pi/4$ is the complete phase from the turning point $r=r_{00}$ to the magnetotail boundary $r=r_m$. If the boundary is

adjoined by the transparency region for SMS waves, then $r_{00}=r_0$, and if it is adjoined by the transparency region for FMS, then $r_{00}=0$ for $m=0$ or $r_{00}=r_{01}$ for $m\neq 0$.

Let us match the internal solution in the magnetosphere to the external solution describing the structure of the oscillations in the solar wind. Let us regard the magnetotail boundary as a tangential discontinuity at $r=r_m$. Note that this approximation, definable as "local", sees the dispersion properties of the oscillations determined by the parameters of the medium directly adjoining the boundary from the inside and outside. In this case the result does not depend on the variation of the medium properties far from the tangential discontinuity. The matching condition (11) serves to obtain a dispersion equation, which we will write down in the following dimensionless form:

$$b\frac{c^2-1}{\varepsilon^{-2}(c^2-M_A^2)-1} = \begin{cases} -\sqrt{k_{rm}^2/k_{rw}^2} & \text{for } \mathrm{Re}(k_{rm}^2),\mathrm{Re}(k_{rw}^2)<0,\\ i\sqrt{-k_{rm}^2/k_{rw}^2} & \text{for } \mathrm{Re}(k_{rm}^2)<0,\mathrm{Re}(k_{rw}^2)>0,\\ -\cot(\psi)\sqrt{-k_{rm}^2/k_{rw}^2} & \text{for } \mathrm{Re}(k_{rm}^2)>0,\mathrm{Re}(k_{rw}^2)<0,\\ i\cot(\psi)\sqrt{k_{rm}^2/k_{rw}^2}, & \text{for } \mathrm{Re}(k_{rm}^2),\mathrm{Re}(k_{rw}^2)>0, \end{cases} \quad (18)$$

where $b=B_{0m}^2/B_{0w}^2$, $c=\overline{\omega}/k_z v_{Am}$ is the dimensionless phase velocity, $M_A=v_0/v_{Am}$ is the Mach number determined by Alfvén speed v_{Am}. In the same notations

$$k_{rm}^2=k_z^2\left(\frac{c^4}{c^2(1+\beta_m^*)-\beta_m^*}-1-\kappa_m^2\right),$$

$$k_{rw}^2=k_z^2\left(\varepsilon^{-2}\frac{(c-M_A)^4}{(c-M_A)^2(1+\beta_w^*)-\varepsilon^2\beta_w^*}-1-\kappa_m^2\right),$$

where $\beta_{m,w}^*=v_{s(m,w)}^2/v_{A(m,w)}^2$, $\kappa_m=m/k_z r_b$, $\varepsilon=v_{Aw}/v_{Am}$ (assuming $v_{Aw}\ll v_{Am}$). To find the solution to the dispersion Eq. (18), let us use the perturbation technique with small-parameter expansion ($\varepsilon\ll 1$)

$$c=c_0+\varepsilon c_1+\cdots. \quad (19)$$

In the zero order of the perturbation theory we have $c_0=M_A$. In the first order of the perturbation theory, squaring the left- and right-hand sides of (18) produces an equation for c_1:

$$\overline{b}^2(M_A^2-1)^2\left(\frac{c_1^4}{c_1^2(1+\beta_w^*)-\beta_w^*}-1-\kappa_m^2\right)=\pm(c_1^2-1)^2k_{rm0}^2, \quad (20)$$

where $k_{rm0}^2\equiv k_{rm}^2(c_0=M_A)$. The plus sign in the right-hand side and $\overline{b}=b$ correspond to $\mathrm{Re}(k_{rm}^2)<0$, the minus sign and $\overline{b}=b\tan(\psi+\pi/4)$ to $\mathrm{Re}(k_{rm}^2)>0$. Eq. (20) is a sixth-order equation with respect to c_1 and its solution can be found numerically. If, however, $|c_1|\gg 1$ (but $\varepsilon|c_1|\ll c_0$) it can be reduced to an approximate biquadratic equation

$$c_1^4\mp c_1^2\frac{\overline{b}^2(M_A^2-1)^2}{k_{rm0}^2(1+\beta_w^*)}\pm\frac{\overline{b}^2}{k_{rm0}^2}(1+\kappa_m^2)(M_A^2-1)^2=0. \quad (21)$$

The solution of (21) for $\mathrm{Re}(k_{rm}^2)<0$ is

$$c_1^2=\frac{b^2(M_A^2-1)^2}{2k_{rm0}^2(1+\beta_w^*)}\pm\sqrt{\frac{b^4(M_A^2-1)^4}{4k_{rm0}^4(1+\beta_w^*)^2}-\frac{b^2(M_A^2-1)^2(1+\kappa_m^2)}{k_{rm0}^2}}. \quad (22)$$

Obviously, the condition $|c_1|\gg 1$ is satisfied when $b\gg 1$ and $|M_A^2-1|\gtrsim 1$. The value of

$$k_{rm0}^2=k_z^2\left(\frac{M_A^4}{M_A^2(1+\beta_m^*)-\beta_m^*}-1-\kappa_m^2\right)$$

is real and hence unstable oscillations are absent when $k_{rm0}^2>0$ ($c_1^2>0$), and the solution for the unstable mode is obtained for $k_{rm0}^2<0$ if the minus sign is chosen before the radical in (22). It is easy to verify that $k_{rm0}^2<0$ for $M_A<M_0$ and $M_1<M_A<M_2$, where $M_0^2=\beta_m^*/(1+\beta_m^*)$, and $M_{1,2}^2$ are the roots of a biquadratic (with respect to M_A) equation $k_{rm0}^2=0$:

$$M_{1,2}^2=\frac{(1+\kappa_m^2)(1+\beta_m^*)}{2}\pm\sqrt{\frac{(1+\kappa_m^2)^2(1+\beta_m^*)^2}{4}-\beta_m^*(1+\kappa_m^2)}.$$

When $\beta_m^*\ll 1$ we have $M_1^2\approx M_0^2+M_0^4/M_2^2<1$ and $M_2^2\approx(1+\kappa_m^2)(1+\beta_m^*)>1$. One can see from the second equation in (18) that, when $\mathrm{Re}(k_{rw}^2)>0$ (corresponding to the transparency region in the solar wind) the value c_1^2 cannot be real, contradicting the solution (22) for $k_{rm0}^2<0$. In this case unstable oscillations are absent. In the case of $\mathrm{Re}(k_{rw}^2)<0$, which corresponds to the first equation in (18), the signs in the left- and right-hand parts of the equation coincide only for $M_A>1$. Hence, when $\mathrm{Re}(k_{rm}^2)<0$, the unstable oscillations are driven on the magnetotail boundary in the parameter range of a shear flow

$$1<M_A<M_2. \quad (23)$$

This conclusion fully agrees with the one in McKenzie (1970b).

The solution of (21) for $\mathrm{Re}(k_r^2)>0$ far from the poles ($\overline{b}^2=\infty$) and zeros ($\overline{b}^2=0$) of the function $\overline{b}=b\tan(\psi+\pi/4)$ is

$$c_1^2=-\frac{\overline{b}^2(M_A^2-1)^2}{2k_{rm0}^2(1+\beta_w^*)}\pm\sqrt{\frac{\overline{b}^4(M_A^2-1)^4}{4k_{rm0}^4(1+\beta_w^*)^2}+\frac{\overline{b}^2(M_A^2-1)^2(1+\kappa_m^2)}{k_{rm0}^2}}. \quad (24)$$

As well as in the $k_{rm0}^2<0$ case, solutions corresponding to the transparency region in the solar wind ($\mathrm{Re}(k_{rw}^2)>0$) describe only steady-state oscillations. Unstable solutions can be found for $k_{rm0}^2>0$, which corresponds to the parameter ranges $M_0<M_A<M_1$ and $M_A>M_2$. The structure of the increment of unstable oscillations is determined by the eigen-values of the phase velocity $c=c_{0n}$ corresponding to the magnetosonic waveguide modes ($\tan(\psi(c_{0n})+\pi/4)=0$, $n=1,2,3\ldots$). These waves propagate in the waveguide adjoining the magnetotail boundary. When $M_A>M_2$, only positive branches of the function $\tan(\psi(M_A)+\pi/4)$ correspond to unstable solutions: $\overline{b}(M_A)=b\tan(\psi(M_A)+\pi/4)>0$, and

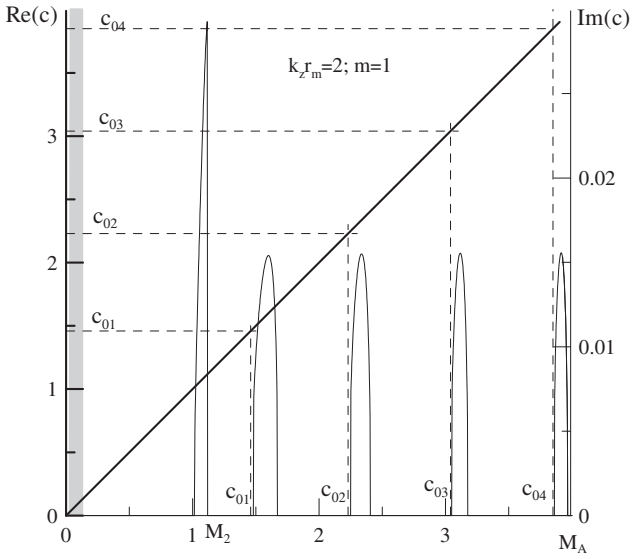

Fig. 3. Mach number M_A dependence of the phase velocity (Re (c), thick line) and the increment (Im (c), thin lines) of unstable oscillations of the magnetotail boundary (in the form of tangential discontinuity) in the WKB approximation over the radial r coordinate. $c_{01,02,03,04}$ are the roots of the dispersion equation $\tan(\psi(c_{0n})+\pi/4)=0$ determining eigen-values c_{0n} for the FMS modes of a waveguide adjoining the magnetotail boundary from the inside. The vertical grey band is the range of the Mach numbers corresponding to possible regimes of the solar wind plasma flow around the Earth's magnetosphere.

when $M_0 < M_A < M_1 < 1$ only negative branches do: $\overline{b}(M_A) = b\tan(\psi(M_A)+\pi/4) < 0$. The first of these ranges ($M_A > M_2$) corresponds to an FMS transparency region adjoining the magnetotail boundary, while the second ($M_0 < M_A < M_1$) to an SMS transparency region. It is possible to show that, near the poles and zeros of the function $\overline{b}(M_A)$, the solutions describe steady-state oscillations (Im $(c) < 0$) only.

Fig. 3 illustrates an example of a numerical solution to the dispersion Eq. (18) for the azimuthal harmonic $m=1$, longitudinal wave vector component $k_z r_m = 2$ and the following parameters of the medium: $\varepsilon = A_w/A_m = 0.08$, $\beta_m^* = 0.005$, $b = B_{0m}^2/B_{0w}^2 = 16$. Notably, no eigen-mode is present in the SMS waveguide. Therefore, the magnetotail is in steady state for $M_A < 1$. When $M_A > 1$ the oscillations under study are unstable in the range (23), as well as in the intervals corresponding to the solutions of (24) above. Each of these roots corresponds to one of the eigen-harmonics of the FMS waveguide adjoining the internal boundary of the magnetotail. When M_A increases, higher and higher harmonics become unstable. It is evident from Fig. 3 that there is no discernible dependence between M_A and the maximum magnitudes of the oscillation increment. However, the range width of the unstable oscillations decreases when M_A (or the number of the eigen-harmonic n) increases.

4. Instability of a magnetotail with a smooth boundary

Let us now consider the problem of boundary stability in an inhomogeneous magnetotail with its boundary in the form of a smooth transition layer. In this case, (9) can only be solved numerically. To obtain a numerical solution and compare it with the above results let us rewrite it in a dimensionless form

$$\frac{\partial}{\partial x}\frac{\tilde{b}^2(x)(\overline{\omega}_A^2(x)-1)}{x\kappa^2(x)}\frac{\partial x\zeta}{\partial x}+(k_z r_m)^2\tilde{b}^2(x)(\overline{\omega}_A^2(x)-1)\zeta = 0, \tag{25}$$

where $x = r/r_m$, $\overline{\omega}_A(x) = [c - M_A\tilde{v}_0(x)]/\tilde{v}_A(x)$, $\tilde{v}_A(x) = v_A(x)/v_{Am}$, $\tilde{v}_0(x) = v_0(x)/v_{0m}$, $\tilde{b}(x) = B_0^2(x)/B_{0m}^2$,

$$\kappa^2(x) = \frac{\overline{\omega}_A^4}{\overline{\omega}_A^2(x)(1+\beta^*(x))-\beta^*(x)} - 1 - \frac{\kappa_m^2}{x^2},$$

$\beta^*(x) = v_A^2(x)/v_s^2(x)$. Let us simulate the profiles of the shear flow velocity $\tilde{v}_0(x)$, Alfvén speed $\tilde{v}_A(x)$ and square of magnetic field strength $\tilde{b}(x)$ using the following functions:

$$\tilde{v}_0(x) = \frac{1}{2}\left[1+\tanh\frac{x-1}{\Delta}\right],$$

$$\tilde{v}_A(x) = \frac{1}{2}\left[\varepsilon+\varepsilon_0+(1-\varepsilon_0)\sqrt{x}+(\varepsilon+\varepsilon_0-(1-\varepsilon_0)\sqrt{x})\tanh\frac{x-1}{\Delta}\right],$$

$$\tilde{b}(x) = \frac{1}{2}\left[1+b^{-1}-(1-b^{-1})\tanh\frac{x-1}{\Delta}\right],$$

where $\Delta = \Delta_r/r_m$, $\varepsilon = v_{Aw}/v_{Am}$, $\varepsilon_0 = v_A(0)/v_{Am}$, $b = B_{0m}^2/B_{0w}^2$, and let us determine the $\beta^*(x)$ function from the plasma configuration equilibrium condition (5):

$$\beta^*(x) = \frac{\beta_m^*}{\tilde{b}(x)} + \frac{\gamma}{2}\left(\frac{1}{\tilde{b}(x)}-1\right).$$

Numerical calculations involved the following magnitudes of the dimensionless parameters: $\Delta = 0.066$, $b = 16$, $\varepsilon_0 = 0.016$, $\varepsilon = 0.008$, $\beta_m^* = 0.005$. What was to be solved was a boundary-value problem of finding the oscillation phase velocity (parameter c, in the dimensionless variables) satisfying the boundary condition (13) when $x \to \infty$, and the finiteness condition when $x \to 0$. The latter requirement means that the solution of (9) must coincide with the solution of the approximate equation

$$r^2\zeta'' + r^\sigma\zeta' + (k_{r0}^2 r^2 - 1)\zeta = 0$$

obtained from (9) when $r \to 0$. Here $k_{r0}^2 \equiv k_r^2(r \to 0)$ (for $m \neq 0$ we have $k_{r0}^2 \approx -m^2/r^2$), and the σ parameter is: $\sigma = 1$ for $m = 0$ and $\sigma = 3$ for $m \neq 0$. The solution which is finite when $r \to 0$ is

$$\zeta = C\begin{cases} J_1(\sqrt{k_{r0}^2}\,r) & \text{for } m = 0, \\ r^{m-1} & \text{for } m \neq 0, \end{cases} \tag{26}$$

where C is the arbitrary constant, $J_1(\sqrt{k_{r0}^2}\,r)$ is the Bessel function: $(J_1(\sqrt{k_{r0}^2}\,r) \overset{r\to 0}{\approx} \sqrt{k_{r0}^2}\,r/2)$. The results of numerical calculations for the increment of unstable oscillations for the azimuthal harmonic $m=1$ and longitudinal wave number $k_z r_m = 2$ are presented in Fig. 4. Comparison with Fig. 3, presenting the solution of the same problem in the local approximation for oscillations in a magnetotail model with a sharp boundary, demonstrates essential differences in the distribution of the oscillation increment.

It should be noted that the solution for the magnetotail with a smooth boundary for $M_A > M_2$ comprises a "bundle" of curves in the $c(M_A)$ plot, which diverge from the basic value $c \approx M_A$ (the zero approximation solution in the previous section) after passing through the eigen-values Re $(c) = c_{0n}$. The solutions were found by a numerical integration of (25) while searching for values of c corresponding to the boundary conditions.

Fig. 4 presents the solutions in the range $0 < M_A < 4$ for harmonics $n = 1,2,3$. Comparison with Fig. 3 shows a manifold decrease of the increment of unstable oscillations, with only some first harmonics (in our case $n = 1,2$) still remaining unstable. This can be explained by the smoothing of the boundary layer and competition between the oscillation dissipation on the resonance surfaces and the shear flow instability. The eigen-value points c_{0n} are also displaced (c_{0n} and M_2 in Fig. 4 are the same points as those obtained by the WKB approximation in Fig. 3), the first region of the unstable oscillations expands.

Fig. 5a illustrates the spatial structure of unstable oscillations close to the second harmonic $n=2$. As has been expected from the analysis of the WKB solution, the solar wind is an opacity region

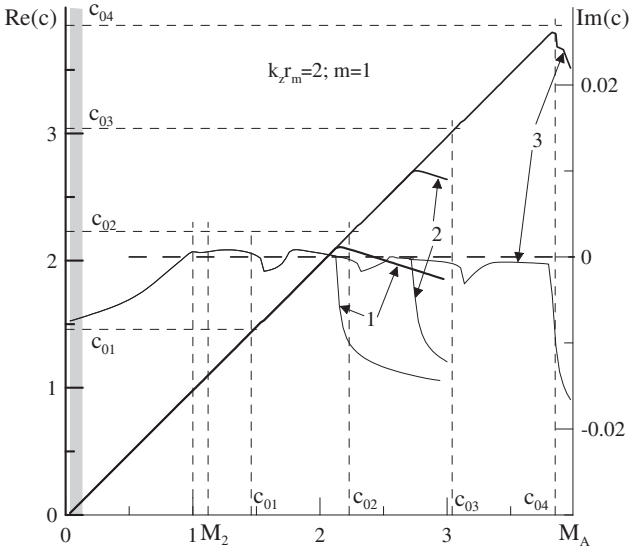

Fig. 4. Mach number M_A dependence of the phase velocity (Re (c), thick line) and the increment (Im (c), thin lines) of the eigen-oscillations of the magnetotail "smooth" boundary with characteristic thickness $\Delta \equiv \Delta_r/r_m = 0.066$. A numerical solution is obtained to (25) for the same parameters of the medium as in Fig. 3. The vertical grey band is the range of the Mach numbers corresponding to possible regimes of the solar wind plasma flow around the Earth's magnetosphere.

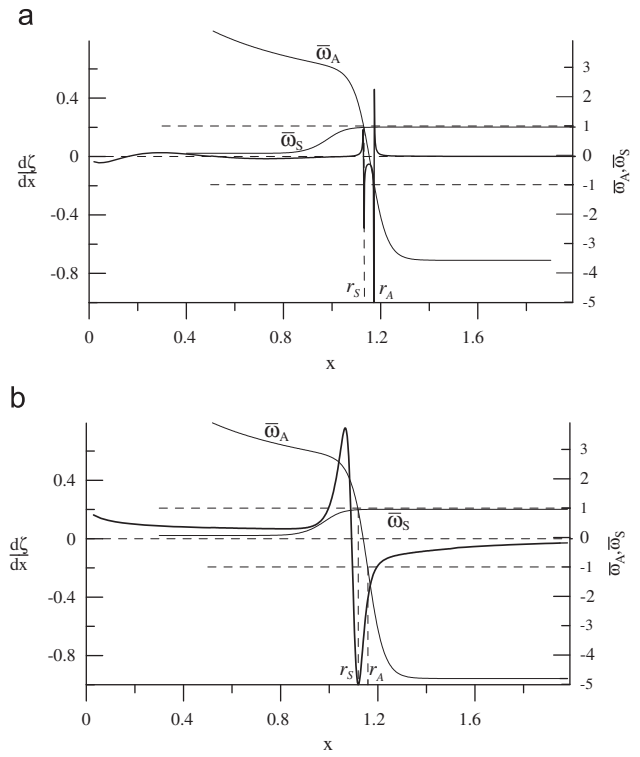

Fig. 5. Spatial structure of the unstable oscillations of the azimuthal harmonic $m=1$: (a) oscillations close to the second harmonic of FMS waves ($n=2$) propagating in the magnetotail waveguide, (b) oscillations of the "global mode" for $k_z r_m \to 0$. Resonance surfaces for the Alfvén and for SMS wave are determined by the points $\overline{\omega}_A(r_A) = \pm 1$ and $\overline{\omega}_A(r_S) = \pm \overline{\omega}_s(r_S)$ (the $\pm$ signes correspond to the signs of the phase velocity of the waves).

for the unstable mode of the oscillations. Resonance surfaces for the Alfvén and SMS waves, determined, respectively, by the conditions $\overline{\omega}_A(r_A) = \pm 1$ and $\overline{\omega}_A(r_S) = \pm \overline{\omega}_s(r_S)$, are located in the magnetotail boundary transition layer.

Note that the value range $M_A > 1$ is never reached for any velocities of the real solar wind flow observed near the Earth's magnetosphere. Therefore, the above analysis implies that the magnetotail boundary always remains locally steady-state. It will be shown below, however, that there is yet another type of unstable magnetotail oscillations remaining unstable for any, however, small, magnitude of the solar wind plasma flow velocity around the magnetosphere.

5. Instability of magnetotail global modes

Fig. 6 presents the increment distribution for yet another type of unstable MHD oscillations in the magnetotail. Their existence does in no way result from the above WKB calculations for the local instability of the magnetotail boundary. They have a rather peculiar spatial structure as shown in Fig. 5b, its prominent feature being that the first derivative $d\zeta/dr$ is practically constant over the radius of the plasma cylinder. As is implied by (6)–(8), this means that the amplitude of such oscillations weakly varies over the magnetotail cross-section. Such oscillations may be defined as "global modes". The following features of these oscillations attract our attention:

1. The $\mathrm{Im}(c(M_A))$ plots for harmonics $m \neq 0$ do not depend on $k_z r_m$ when $k_z r_m \to 0$.
2. When M_A increases, the increment of the oscillations decreases and tends to zero for azimuthal harmonics $m \neq 0$ when $M_A = M_{Ac}$ (the magnitude of M_{Ac} is different for various m).

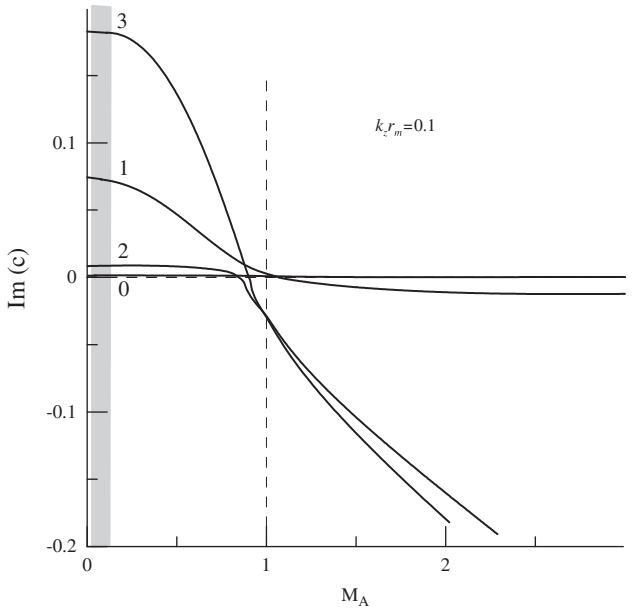

Fig. 6. Mach number M_A dependence of the magnetotail "global mode" increment for the azimuthal harmonics $m=0,1,2,3$ ($k_z r_m=1$). The vertical grey band is the range of the Mach numbers corresponding to possible regimes of the solar wind plasma flow around the Earth's magnetosphere.

3. For oscillations with $m=0$ the $\mathrm{Im}(c(M_A))$ plots differ essentially for oscillations with various $k_z r_m$, having no restricting value of M_{Ac} to terminate the region of existence of unstable oscillations.
4. The absolute values of the increment for the harmonics $m \neq 0$ are much larger than for the harmonic $m=0$.

To qualitatively analyse these features of the global modes, let us consider the following simplified model for $k_z r_m \to 0$. This means that the second derivative of ζ may be neglected in (9):

$$\left(\nabla_r \ln\left(\frac{\rho_0\Omega^2}{k_r^2}\right) + r^{-1}\right)\frac{\partial\zeta}{\partial r} + \left(k_r^2 + r^{-1}\nabla_r \ln\left(\frac{\rho_0\Omega^2}{k_r^2 r}\right)\right)\zeta \approx 0.$$

The solution of this equation is

$$\zeta = C\exp\left(-\int_{r_b}^{r}\frac{k_r^2 r' + \nabla_{r'}\ln(\rho_0\Omega^2/k_r^2 r')}{r'\nabla_{r'}\ln\left(\rho_0\Omega^2/k_r^2\right)+1}dr'\right),$$

where C is an arbitrary constant. When $k_z r_m \ll 1$ the solar wind is an opacity region for global modes with $m \neq 0$. The matching condition (11) yields the following dispersion equation:

$$-\frac{\rho_{0w}\Omega_w^2}{\sqrt{-k_{rw}^2}} = \frac{\rho_{0m}\Omega_m^2}{k_{rm}^2}\left(r_m^{-1} - \frac{k_{rm}^2 + r_m^{-1}\nabla_r\ln(\rho_0\Omega^2/k_r^2 r_m)}{\nabla_r\ln(\rho_{0m}\Omega_m^2/k_{rm}^2) + r_m^{-1}}\right).$$

As an estimate, let us set $|\nabla_r \ln(\rho_{0m}\Omega_m^2/k_{rm}^2)| \lesssim r_m^{-1}$ in the square brackets. Or, in the dimensionless form

$$\frac{(c-M_A)^2/\varepsilon^2 - 1}{\sqrt{-k_{rw}^2/k_z^2}} = \frac{b(c^2-1)}{k_z r_m}\left[(k_z r_m)^2 - \frac{k_z^2}{k_{rm}^2}\right], \tag{27}$$

where

$$k_{rw}^2 = k_z^2\left(\frac{(c-M_A)^4/\varepsilon^4}{(c-M_A)^2(1+\beta_w)/\varepsilon^2 - \beta_w} - 1 - \kappa_m^2\right),$$

$$k_{rm}^2 = k_z^2\left(\frac{c^4/}{c^2(1+\beta_m)-\beta_m} - 1 - \kappa_m^2\right),$$

$b = B_{0m}^2/B_{0w}^2 > 1$, $\varepsilon = v_{Aw}/v_{A_m} \ll 1$, $\kappa_m = m/k_z r_m$. Let us seek a solution to (27) in accordance with the perturbation theory in the form of expansion (19) over the small parameter ε. In the zero

approximation we have $c_0=M_A$. The first order of the perturbation theory yields

$$c_1^2 \approx b(M_A^2-1)(m+m^{-1})+1. \quad (28)$$

This solution describes an unstable mode ($c_1^2<0$) when $M_A<M_{Ac}$, where

$$M_{Ac}=\sqrt{1-\frac{m}{b(m^2+1)}}.$$

Thus it is evident that the instability increment (28) in the limiting case $k_z r_m \to 0$ does not depend on $k_z r_m$. The instability range is restricted by the requirement $0<M_A<M_{Ac}$ in full agreement with the above-noted features of the unstable global modes with $m\neq 0$ in items 1–2.

It will be evident from the subsequent calculations that the solar wind is a transparency region for global mode with $m=0$ in the same limiting case $k_z r_m \ll 1$. Let us use the matching condition (11) to obtain the following dispersion equation:

$$i\frac{(c-M_A)^2/\varepsilon^2-1}{\sqrt{k_{rw}^2/k_z^2}}=\frac{b(c^2-1)}{k_z r_m}\left[(k_z r_m)^2-\frac{k_z^2}{k_{rm}^2}\right]. \quad (29)$$

In the zeroth order of the perturbation theory, we have again $c_0=M_A$. In the first order we obtain the following approximate expression:

$$c_1 \approx i\frac{b}{k_z r_m}\frac{(M_A+1)(M_A^2-M_0^2)}{(M_A-\beta_m^*)\sqrt{1+\beta_w^*}},$$

where $M_0^2=\beta_m^*/(1+\beta_m^*)$. It is easily verifiable that the mode in question is unstable ($\mathrm{Im}\ (c_1)>0$) throughout the M_A variation range, except for a narrow interval, $M_0<M_A<\beta_m^*$. This is consistent with the features of the unstable global mode with $m=0$ as noted above in items 3 and 4.

Note that the thus obtained solutions should be regarded as an illustration only of the qualitative behaviour of global modes. The exact values of their increment as obtained numerically may differ considerably from these simplified estimates.

Fig. 7 plots the increment versus the frequency of unstable global modes with $m=0$ and $m=1$ for various velocities of the solar wind flowing round the magnetosphere. The calculations have been carried out numerically for parameter $k_z r_m$ varying $0\le k_z r_m \le 8$. One's attention is attracted both to the difference in the qualitative behaviour of these harmonics, as well as to their absolute values—the increments for harmonic $m=1$ are several times as large as those for harmonic $m=0$.

Fig. 8 plots the frequency dependences of the global mode increment for the azimuthal harmonics $m=1,2\ldots$, 5 for various velocities of the plasma flow around the magnetosphere. The oscillation increment increases with the azimuthal wave number. Negative frequencies $f=\mathrm{Re}(\omega)/2\pi<0$ correspond to the unstable upstream waves whose parallel phase velocity $\mathrm{Re}\ (\omega)/k_z$ is directed along the solar wind flowing round the magnetosphere, whereas the positive ones $f=\mathrm{Re}(\omega)/2\pi>0$ to the downstream waves. When the velocity of the plasma flow around the magnetosphere increases, the frequency interval of the unstable downstream waves decreases.

The above discussed unstable global modes in the magnetotail cover the frequency range corresponding to ultra-low-frequency (~ 1 mHz) MHD oscillations observed in the Earth's magnetosphere. In particular, they can be the source of eigen-oscillations in the resonator in the near-Earth part of the plasma sheet (Leonovich and Mazur, 2005; Mazur and Leonovich, 2006). The eigen-modes of this resonator are observable as ultra-low-frequency oscillations with a discrete frequency spectrum (so-called magic frequencies 0.8, 1.1, 1.3, 1.6…mHz—Ruohoniemi et al., 1991; Samson and Harrold, 1992). Their localization area as projected onto the Earth's surface ranges 60°–80° latitude in the Northern hemisphere—Mathie et al. (1999) and Wanliss et al. (2002). This means that such oscillations occupy most of the magnetotail cross-section in the magnetosphere. Thus, unstable global modes may be considered as a potential source of eigen-oscillations of the resonator in the near-Earth part of the plasma sheet.

6. Conclusion

Here is a list of the main results of this work.

1. An Eq. (9) is obtained describing the MHD oscillations in the magnetotail, simulated using a model plasma cylinder within the solar wind plasma flow. Its solution (9) is analytically found in the WKB approximation over the radial coordinate for the plasma cylinder with its boundary having the form of a tangential discontinuity. It is shown that the boundary is unstable, with respect to the fast magnetosonic oscillations, for the range of the flow parameters $1<M_A<M_2$ (where $M_A=v_0/v_{Am}$ is the Mach number specified by the Alfvén velocity on the magnetotail boundary, $M_0<M_1<1$; $M_2>1$ are the characteristic Mach numbers determined in Section 3). The boundary of the plasma cylinder is also unstable near the eigen-values $M_A=c_{0n}=\mathrm{Re}((\omega_n/k_z v_{Am}))$ determined by the dispersion equation for the magnetosonic waves travelling through the magnetospheric waveguide: $\tan(\psi(c_{0n})+\pi/4)=0$, $n=1,2,3\ldots$, where ψ is the spatial oscillation phase digitized from the turning point to the plasma cylinder boundary, (ω_n/k_z) is parallel phase velocity of the n-th harmonic of the oscillations.

A numerical solution of the problem for the model magnetotail with a smooth boundary layer has demonstrated that the range of

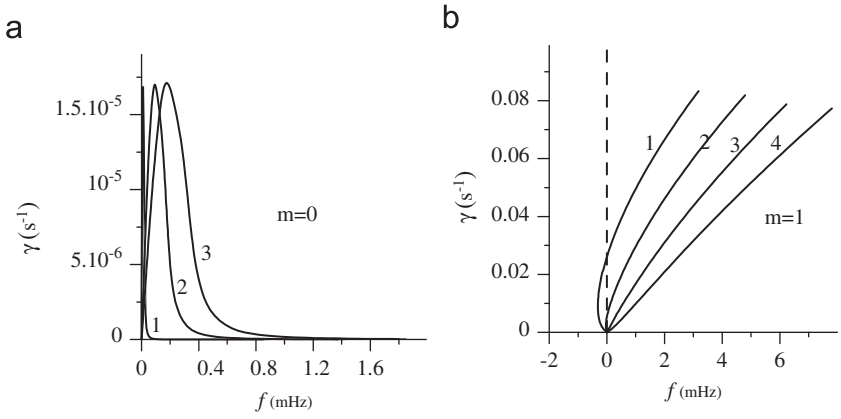

Fig. 7. Frequency $f=k_z v_{Am}\mathrm{Re}(c)/2\pi$ dependence of the "global mode" increment $\gamma=k_z v_{Am}\mathrm{Im}(c)$ for the azimuthal harmonics (a) $m=0$ and (b) $m=1$ for various velocities of the solar wind plasma flow around the magnetotail: (1) $v_0=200$ km/s, (2) $v_0=400$ km/s, (3) $v_0=600$ km/s, (4) $v_0=800$ km/s.

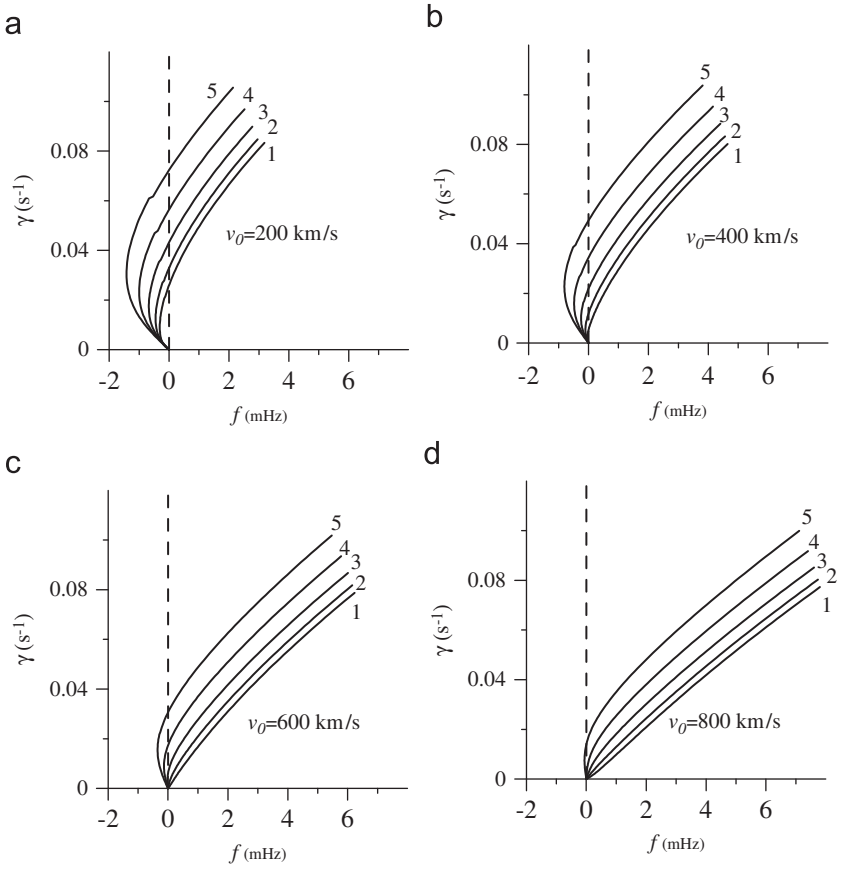

Fig. 8. Frequency $f=k_z v_{Am}\mathrm{Re}(c)/2\pi$ dependence of the "global mode" increment $\gamma=k_z v_{Am}\mathrm{Im}(c)$ for the azimuthal harmonics $m=1,2\ldots,5$ for various velocities of the solar wind plasma flow around the magnetotail: (a) $v_0=200$ km/s, (b) $v_0=400$ km/s, (c) $v_0=600$ km/s, (d) $v_0=800$ km/s.

M_A values for which the boundary becomes unstable is consistent with the results of the WKB approximation. There are significant differences, however. The absolute values of the unstable oscillation increment for the tail with a smooth boundary layer are much smaller than those for the tail with a sharp boundary. This may be explained by both boundary layer smoothing, and competition between the shear flow instability and dissipation of the oscillation energy on the resonance surfaces for the Alfvén and SMS waves.

For the actually observed velocities of the solar wind plasma flows around the Earth's magnetosphere, $M_A<1$. Therefore, the magnetotail boundary always remains locally steady-state.

2. New unstable "global modes" of magnetotail oscillations have been discovered. Their amplitude varies little across the tail. These modes remain unstable for any, however, slow velocity of the solar wind flow round the magnetosphere. The increment distribution of the global modes differs substantially between the axisymmetric ($m=0$) and asymmetric ($m\neq 0$) azimuthal harmonics. The region of existence for unstable asymmetrical modes occupies the range $0<M_A<M_{Ac}$, where M_{Ac} is the limiting magnitude of M_A up to which they remain unstable. When $k_z r_m\to 0$ the increment distribution of such oscillations is directly proportional to $k_z r_m$. Axisymmetric global modes remain unstable for any Mach number M_A. Their increment is much smaller than the increment of asymmetric modes.

The typical frequencies of unstable global modes in the magnetotail are within the range of the lowest-frequency MHD oscillations observable in the Earth's magnetosphere (~ 1 mHz). The resonator eigen-modes in the near-Earth plasma sheet fit into this ("magic frequency") range. Instability of the global modes may be the source of pumping the first harmonics in this resonator.

Note that these results were obtained for a magnetotail model in the form of a radially inhomogeneous plasma cylinder. This model cannot take into account such features of the real magnetotail as the presence of the plasma sheet dividing it into two lobes with oppositely directed magnetic field. To take these features into account it is necessary to use more complicated two- or three-dimensionally inhomogeneous models. Hopefully, the solutions obtained here for the unstable MHD modes will be valid for those models, even though their increment will undoubtedly differ essentially from the increment in this work.

Acknowledgements

This work was partially supported by RFBR Grant #09-02-00082 and by Program #4 of the Presidium of the Russian Academy of Sciences and OFN RAS #15.

Appendix A. Derivation of the basic equation (9)

Let us linearize and write down the components of Eqs. (1), (2) and (4):

$$-i\overline{\omega}\rho_0 v_r=-\nabla_r P+\frac{B_0}{\mu_0}(ik_z B_r-\nabla_r B_z)-\frac{B_z}{\mu_0}\nabla_r B_0, \tag{A.1}$$

$$-i\overline{\omega}\rho_0 v_\phi=-i\frac{m}{r}P-i\frac{B_0}{\mu_0}\left(\frac{m}{r}B_z-k_z B_\phi\right), \tag{A.2}$$

$$-i\overline{\omega}\rho_0 v_z=-\rho_0 v_r\nabla_r v_0-ik_z P+\frac{B_r}{\mu_0}\nabla_r B_0, \tag{A.3}$$

$$-i\overline{\omega}B_r = ik_zB_0v_r, \tag{A.4}$$

$$-i\overline{\omega}B_\phi = ik_zB_0v_\phi, \tag{A.5}$$

$$-i\overline{\omega}B_z = \frac{1}{r}\nabla_r r(v_0B_r - v_rB_0) + i\frac{m}{r}(v_0B_\phi - v_\phi B_0), \tag{A.6}$$

$$-i\frac{\overline{\omega}}{\rho_0}P = -v_s^2\left(\frac{1}{r}\nabla_r rv_r + i\frac{m}{r}v_\phi + ik_zv_z\right) - v_r\frac{1}{\rho_0}\frac{dP_0}{dr}, \tag{A.7}$$

where $v_s = \sqrt{\gamma P_0/\rho_0}$ is sound velocity in plasma. From (A.4) and (A.5) we have

$$B_r = -\frac{k_zB_0}{\overline{\omega}}v_r, \tag{A.8}$$

$$B_\phi = -\frac{k_zB_0}{\overline{\omega}}v_\phi. \tag{A.9}$$

Substituting (A.8) and (A.9) into (A.2) and (A.6), we obtain

$$v_\phi K_A^2 = \frac{m}{r\rho_0\overline{\omega}}P + \frac{mB_0}{\mu_0\rho_0\overline{\omega}r}B_z,$$

$$B_z = -i\frac{1}{r}\nabla_r\left(\frac{rB_0}{\overline{\omega}}v_r\right) + \frac{mB_0}{r\overline{\omega}}v_\phi,$$

where $K_A^2 = 1 - k_z^2v_A^2/\overline{\omega}^2$, $v_A = B_0/\sqrt{\mu_0\rho_0}$ is the Alfvén speed. Hence we obtain

$$v_\phi = K_s^{-2}\left[-i\frac{mv_A^2}{\overline{\omega}r^2}\nabla_r\left(\frac{r}{\overline{\omega}}v_r\right) - i\frac{mB_0\nabla_r(B_0)}{r\mu_0\rho_0\overline{\omega}^2}v_r + \frac{m}{r\rho_0\overline{\omega}}P\right], \tag{A.10}$$

$$B_z = -i\frac{K_A^2}{K_s^2r}\nabla_r\left(\frac{rB_0}{\overline{\omega}}v_r\right) + \frac{m^2B_0}{r^2\overline{\omega}^2\rho_0K_s^2}P, \tag{A.11}$$

where $K_s^2 = K_A^2 - m^2v_A^2/r^2\overline{\omega}^2$. Expressing v_z from (A.3) and substituting the obtained expression and (A.10) into (A.7), we obtain

$$P = -i\frac{K_A^2\rho_0v_s^2}{\chi_S^2\overline{\omega}}\left[\frac{1}{r}\nabla_r(rv_r) + \left(\frac{k_z\nabla_r(v_0)}{\overline{\omega}} + \left(1 - K_s^2\left(1 + \frac{v_A^2}{v_s^2K_A^2}\right)\right)\nabla_r(\ln B_0)\right)v_r\right], \tag{A.12}$$

where $\chi_S^2 = 1 - (k_z^2 + m^2/r^2)(v_A^2 + v_s^2 - k_z^2v_A^2v_s^2/\overline{\omega}^2)/\overline{\omega}^2$. Expressing now the radial component of the velocity through the displacement $v_r = d\zeta/dt = \partial\zeta/\partial t + (\mathbf{v}_0\nabla)\zeta = -i\overline{\omega}\zeta$ and substituting it into the expression obtained above for the wave field components we obtain (6), (7) and (8). The Eq. (A.1), in view of (A.8) and (A.11), can be rewritten as

$$\frac{1}{\overline{\omega}^2\rho_0}\frac{\partial}{\partial r}\left(P + \frac{B_0B_z}{\mu_0}\right) - K_A^2\zeta = 0,$$

where the expression in brackets $(P + B_0B_z/\mu_0)$ is the full perturbed pressure. Substituting P and B_z from (7) and (8) into this expression we obtain the basic equation (9).

References

Borovsky, J.E., Thomsen, M.F., Elphic, R.C., Cayton, T.E., McComac, D.J., 1998. The transport of plasma sheet material from the distant tail to geosynchronous orbit. J. Geophys. Res. 103, 20297–20331.

Engebretson, M., Glassmeier, K.-H., Stellmacher, M., Hughes, W.J., Luehr, H., 1998. The dependence of high-latitude Pc5 wave power on solar wind velocity and on the phase of high-speed solar wind streams. J. Geophys. Res. 103, 26271–26283.

Fujita, S., Glassmeier, K.-H., Kamide, K., 1996. MHD waves generated by the Kelvin–Helmholtz instability in a nonuniform magnetosphere. J. Geophys. Res. 101, 27317–27326.

Leonovich, A.S., Mazur, V.A., 2005. Why do ultra-low-frequency MHD oscillations with a discrete spectrum exist in the magnetosphere? Ann. Geophys. 23, 1075–1079.

Leonovich, A.S., Mazur, V.A., 2008. Eigen ultra-low-frequency magnetosonic oscillations of the near plasma sheet. Cosmic Res. 46, 327–334.

Leonovich, A.S., Kozlov, D.A., 2009. Alfvénic and magnetosonic resonances in a nonisothermal plasma. Plasma Phys. Control. Fus. 51, 085007. doi:10.1088/0741-3335/51/8/085007.

Mann, I.R., Wright, A.N., 1999. Diagnosing the excitation mechanisms of Pc5 magnetospheric flank waveguide mode and FLRs. Geophys. Res. Lett. 26, 2609–2612.

Mann, I.R., Voronkov, I., Dunlop, M., Donovan, E., et al., 2002. Coordinated ground-based and Cluster observations of large amplitude global magnetospheric oscillations during a fast solar wind speed interval. Ann. Geophys. 20, 405–426.

Mathie, R.A., Menk, F.W., Mann, I.R., Orr, D., 1999. Discrete field line resonances and the Alfvén continuum in the outer magnetosphere. Geophys. Res. Lett. 26, 659–662.

Mazur, V.A., Leonovich, A.S., 2006. ULF hydromagnetic oscillations with the discrete spectrum as eigenmodes of MHD-resonator in the near-Earth part of the plasma sheet. Ann. Geophys. 24, 1639–1648.

McKenzie, J.F., 1970a. Hydromagnetic wave interaction with the magnetopause and the bow shock. Planet. Space Sci. 18, 1–14.

McKenzie, J.F., 1970b. Hydromagnetic oscillations of the geomagnetic tail and plasma sheet. J. Geophys. Res. 75, 5331–5339.

Mills, K.J., Wright, A.N., Mann, I.R., 1999. Kelvin–Helmholtz driven modes of the magnetosphere. Phys. Plasmas 6, 4070–4086.

Rankin, R., Frycz, P., Samson, J.C.V.T., 1997. Shear flow vortices in magnetospheric plasmas. Phys. Plasmas 4, 829–840.

Ruohoniemi, J.M., Greenwald, R.A., Baker, K.B., 1991. HF radar observations of Pc5 field line resonances in the midnight/early morning MLT sector. J. Geophys. Res. 96, 15697–15710.

Samson, J.C., Harrold, B.G., 1992. Field line resonances associated with waveguides in the magnetosphere. Geophys. Res. Lett. 19, 441–444.

Sergeev, V.A., Tsyganenko, N.A. 1980. The Earth's magnetosphere, Moscow, Nauka (in Russian).

Southwood, D.J., 1968. The hydromagnetic stability of the magnetospheric boundary. Planet. Space Sci. 16, 587–605.

Wanliss, J.A., Rankin, R., Samson, J.C., Tikhonchuk, V.T., 2002. Field line resonances in a stretched magnetotail: CANOPUS optical and magnetometer observations. J. Geophys. Res. 107, SMP9,1100. doi:10.1029/2001JA000257.